J|A|C|S ARTICLES

Published on Web 05/14/2009

Accurate Measurement of Methyl ^{13}C Chemical Shifts by Solid-State NMR for the Determination of Protein Side Chain Conformation: The Influenza A M2 Transmembrane Peptide as an Example

Mei Hong,* Tatiana V. Mishanina, and Sarah D. Cady

Department of Chemistry, Iowa State University, Ames, Iowa 50011

Received February 27, 2009; E-mail: mhong@iastate.edu

Abstract: The use of side chain methyl ^{13}C chemical shifts for the determination of the rotameric conformation of Val and Leu residues in proteins by solid-state NMR spectroscopy is described. Examination of the solution NMR stereospecifically assigned methyl groups shows significant correlation between the difference in the two methyl carbons' chemical shifts and the side chain conformation. It is found that α-helical and β-sheet backbones cause different side chain methyl chemical shift trends. In α-helical Leu's, a relatively large absolute methyl ^{13}C shift difference of 2.89 ppm is found for the most populated *mt* rotamer ($\chi_1 = -60°$, $\chi_2 = 180°$), while a much smaller value of 0.73 ppm is found for the next populated *tp* rotamer ($\chi_1 = 180°$, $\chi_2 = 60°$). For α-helical Val residues, the dominant *t* rotamer ($\chi_1 = 180°$) has more downfield Cγ2 chemical shifts than Cγ1 by 1.71 ppm, while the next populated *m* rotamer ($\chi_1 = -60°$) shows the opposite trend of more downfield Cγ1 chemical shift by 1.23 ppm. These significantly different methyl ^{13}C chemical shifts exist despite the likelihood of partial rotameric averaging at ambient temperature. We show that these conformation-dependent methyl ^{13}C chemical shifts can be utilized for side chain structure determination once the methyl ^{13}C resonances are accurately measured by double-quantum (DQ) filtered 2D correlation experiments, most notably the dipolar DQ to single-quantum (SQ) correlation technique. The advantage of the DQ−SQ correlation experiment over simple 2D SQ−SQ correlation experiments is demonstrated on the transmembrane peptide of the influenza A M2 proton channel. The methyl chemical shifts led to predictions of the side chain rotameric states for several Val and Leu residues in this tetrameric helical bundle. The predicted Val rotamers were further verified by dipolar correlation experiments that directly measure the χ_1 torsion angles. It was found that the chemical-shift-predicted side chain conformations are fully consistent with the direct torsion angle results; moreover, the methyl ^{13}C chemical shifts are sensitive to ∼5° changes in the χ_1 torsion angle due to drug binding.

Introduction

Recent advances in extensive ^{13}C and ^{15}N labeling, multidimensional correlation methods, and improved sample preparation protocols that produce well-ordered solid proteins have enabled atomic-level three-dimensional structure determination of proteins by solid-state NMR.[1−5] Despite the tremendous progress, most studies have so far focused on the backbone conformation and fold, with considerably lower resolution structure for the side chains.[6] Side chains are important for enzyme active site chemistry and interaction with small molecules. For ion channels in lipid membranes, the positions of side chains, as manifested by their (χ_1, χ_2) angles, have important implications for ion conduction and transport. In principle, two NMR approaches are available for determining the protein side chain conformation. The first measures the torsion angles by correlating the dipolar couplings along the two bonds sandwiching the torsional bond of interest. For the χ_1 angle, a natural choice is to correlate the Cα−Hα and Cβ−Hβ dipolar couplings.[7,8] However, the dipolar correlation-based torsion angle experiments work best for β-branched residues (Val, Ile, Thr) with a single Hβ proton.[9] For long-chain amino acids where methylene groups dominate, the torsion angle results are less easy to interpret, thus side chain torsion angles farther away from the backbone are harder to measure. The second approach is to measure distances between side chain carbons

(1) Castellani, F.; vanRossum, B.; Diehl, A.; Schubert, M.; Rehbein, K.; Oschkinat, H. *Nature* **2002**, *420*, 98–102.
(2) Franks, W. T.; Zhou, D. H.; Wylie, B. J.; Money, B. G.; Graesser, D. T.; Frericks, H. L.; Sahota, G.; Rienstra, C. M. *J. Am. Chem. Soc.* **2005**, *127*, 12291–12305.
(3) Petkova, A. T.; Yau, W. M.; Tycko, R. *Biochemistry* **2006**, *45*, 498–512.
(4) Wasmer, C.; Lange, A.; Van Melckebeke, H.; Siemer, A. B.; Riek, R.; Meier, B. H. *Science* **2008**, *319*, 1523–1526.
(5) Zech, S. G.; Wand, A. J.; McDermott, A. E. *J. Am. Chem. Soc.* **2005**, *127*, 8618–8626.
(6) Rienstra, C. M.; Tucker-Kellogg, L.; Jaroniec, C. P.; Hohwy, M.; Reif, B.; McMahon, M. T.; Tidor, B.; Lozano-Perez, T.; Griffin, R. G. *Proc. Natl. Acad. Sci. U.S.A.* **2002**, *99*, 10260–10265.
(7) Feng, X.; Lee, Y. K.; Sandstroem, D.; Eden, M.; Maisel, H.; Sebald, A.; Levitt, M. H. *Chem. Phys. Lett.* **1996**, *257*, 314–320.
(8) Feng, X.; Verdegem, P. J. E.; Lee, Y. K.; Sandstrom, D.; Eden, M.; Bovee-Geurts, P.; de Grip, W. J.; Lugtenburg, J.; de Groot, H. J. M.; Levitt, M. H. *J. Am. Chem. Soc.* **1997**, *119*, 6853–6857.
(9) Rienstra, C. M.; Hohwy, M.; Mueller, L. J.; Jaroniec, C. P.; Reif, B.; Griffin, R. G. *J. Am. Chem. Soc.* **2002**, *124*, 11908–11922.

10.1021/ja901550q CCC: $40.75

and backbone atoms such as the amide nitrogen.[10] However, these experiments have limited sensitivity due to the need for long transverse mixing times and as a result have been demonstrated only on well-ordered microcrystalline proteins with long T_2 relaxation times.

In principle, the chemical shifts of side chain carbons should reflect the side chain torsion angles χ_1, χ_2, and so on, analogous to the influence of (ϕ, ψ) torsion angles on backbone ^{13}C chemical shifts.[11,12] Since chemical shifts are much easier to measure than torsion angles and distances, there is a considerable incentive to determine whether a correlation exists between the side chain ^{13}C chemical shifts and the rotameric conformation. Indeed, chemical shielding computation indicated that the χ_1 torsion angle affects the Cγ shielding of Val:[13] the $\chi_1 = 180°$ conformation has a more shielded (upfield) Cγ1 than Cγ2, while the $\chi_1 = -60°$ conformation has a more deshielded (downfield) Cγ1 resonance. A more recent computation study found the Ile Cγ1 and Cγ2 chemical shift anisotropies are sensitive to both (χ_1, χ_2) angles.[14] Very recently, an analysis of side chain ^{13}C chemical shifts of nine amino acids in five proteins showed a correlation between upfield shifts of the Cγ resonances and *gauche* conformations of the γ-substituents.[15] Overall, however, efforts to predict and exploit the conformational dependence of side chain ^{13}C chemical shifts have been quite limited, mainly due to the concern that rotameric averaging may be too extensive for clear chemical shift differences to remain at ambient temperature. The second concern is aromatic ring current effects,[16,17] which can affect the side chain chemical shifts significantly. Third, for double-methyl residues Val, Leu, and Ile, stereospecific assignment of the two methyl carbons is highly desirable if not absolutely necessary to establish a clear correlation between conformation and methyl chemical shifts.

Stereospecific assignment of the two methyl ^{13}C chemical shifts of Val and Leu has been possible by solution NMR for a number of years. One approach uses fractional ^{13}C labeling to create different labeling levels of the two methyl carbons due to their different stereoselective biosynthetic pathways.[18] A second approach measures three-bond J-couplings, $^3J_{CN\gamma}$ and $^3J_{CC\gamma'}$, to give stereospecific assignment of Val residues once the Karplus equations are accurately parametrized.[19−22] With these methods, an increasing database of proteins with known conformation and known methyl ^{13}C chemical shifts has become available. More recently, analyses of side chain C−H residual dipolar couplings (RDCs) in partially aligned media have allowed more precise determination of rotameric populations in proteins.[23,24] These scalar and dipolar coupling measurements showed that many Val, Leu, and Ile residues in globular proteins in solution adopt a single rotameric state with only small fluctuations around the mean, while those that show conformational equilibria between different canonical rotamers often retain one dominant (greater than ∼75%) conformation.

The 2D ^1H-driven ^{13}C spin-diffusion experiment, due to its simplicity and robustness, has become the standard method of choice for ^{13}C-based assignment of solid proteins. For well-ordered proteins with narrow linewidths, these 2D spin-diffusion-based correlation spectra, a variant of which is called DARR,[25] contain surprisingly high levels of information and allow many spin systems to be resolved and assigned. However, the DARR experiment is less useful for membrane peptides and proteins since the high natural abundance signals of the lipids tend to obscure cross peaks near the diagonal. Moreover, membrane proteins usually have broader lines than microcrystalline proteins or fibrous proteins due to conformational and dynamic disorder induced by the lipids. While alternative MAS techniques for 2D homonuclear correlation spectroscopy have been available, direct comparisons among these techniques have not been made, especially for side chain resonance assignment of membrane proteins. Here, we compare the 2D DARR experiment with two double-quantum-filtered (DQF) $^{13}C-^{13}C$ correlation experiments that are equivalent to the solution NMR DQF-COSY experiment[26] and the INADEQUATE experiment,[27,28] for the purpose of accurately measuring methyl ^{13}C chemical shifts to determine protein side chain conformations.

We use the influenza A M2 transmembrane peptide (M2TMP) to demonstrate the accurate measurement of methyl ^{13}C chemical shifts and to verify the correlation between these shifts and the side chain conformation of Val. The M2 protein of influenza A virus forms a proton channel in the virus envelope that is essential for viral replication.[29] Opening of the channel acidifies the viral core, which triggers the release of the viral ribonucleoprotein complex into the host cell.[30] A number of high-resolution structural studies have been carried out on the transmembrane domain of the M2 protein, using X-ray crystallography,[31] solution NMR,[32] oriented solid-state NMR (SSNMR),[33,34] and magic-angle spinning SSNMR.[35,36] Thus, a relatively large amount of structural information is available. Using the methyl

(10) Helmus, J. J.; Nadaud, P. S.; Höfer, N.; Jaroniec, C. P. *J. Chem. Phys.* **2008**, *128*, 052314.
(11) deDios, A. C.; Pearson, J. G.; Oldfield, E. *Science* **1993**, *260*, 1491–1496.
(12) Wishart, D. S.; Sykes, B. D.; Richards, F. M. *J. Mol. Biol.* **1991**, *222*, 311–333.
(13) Pearson, J. G.; Le, H.; Sanders, L. K.; Godbout, N.; Havlin, R. H.; Oldfield, E. *J. Am. Chem. Soc.* **1997**, *119*, 11941–11950.
(14) Sun, H.; Sanders, L. K.; Oldfield, E. *J. Am. Chem. Soc.* **2002**, *124*, 5486–5495.
(15) London, R. E.; Wingad, B. D.; Mueller, G. A. *J. Am. Chem. Soc.* **2008**, *130*, 11097–11105.
(16) Haigh, C. W.; Mallion, R. B. *Prog. Nucl. Magn. Reson. Spectrosc.* **1979**, *13*, 303–344.
(17) Stamm, H.; Jackel, H. *J. Am. Chem. Soc.* **1989**, *111*, 6544–6550.
(18) Neri, D.; Otting, G.; Wuethrich, K. *Tetrahedron* **1990**, *46*, 3287–3296.
(19) Vuister, G. W.; Bax, A. *J. Am. Chem. Soc.* **1993**, *115*, 7772–7777.
(20) Grzesiek, S.; Vuister, G. W.; Bax, A. *J. Biomol. NMR* **1993**, 487–493.
(21) Karimi-Nejad, Y.; Schmidt, J. M.; Rüterjans, H.; Schwalbe, H.; Greisinger, C. *Biochemistry* **1994**, *33*, 5481–5492.
(22) Tugarinov, V.; Kay, L. E. *J. Am. Chem. Soc.* **2004**, *126*, 9827–9836.
(23) Chou, J. J.; Case, D. A.; Bax, A. *J. Am. Chem. Soc.* **2003**, *125*, 8959–8966.
(24) Mittermaier, A.; Kay, L. E. *J. Am. Chem. Soc.* **2001**, *123*, 6892–6903.
(25) Takegoshi, K.; Nakamura, S.; Terao, T. *Chem. Phys. Lett.* **2001**, *344*, 631–637.
(26) Piantini, U.; Sorensen, O. W.; Ernst, R. R. *J. Am. Chem. Soc.* **1982**, *104*, 6800–6801.
(27) Bax, A.; Freeman, R.; Kempsell, S. P. *J. Am. Chem. Soc.* **1980**, *102*, 4849–4851.
(28) Hong, M. *J. Magn. Reson.* **1999**, *136*, 86–91.
(29) Pinto, L. H.; Lamb, R. A. *J. Biol. Chem.* **2006**, *281*, 8997–9000.
(30) Lamb, R. A.; Holsinger, K. J.; Pinto, L. H. The Influenza A Virus M2 Ion Channel Protein and Its Role in the Influenza Virus Life Cycle. In *Cellular Receptors of Animal Viruses*; Wemmer, E., Ed.; Cold Spring Harbor Lab Press: Plainview, NY, 1994; pp 303−321.
(31) Stouffer, A. L.; Acharya, R.; Salom, D.; Levine, A. S.; Di Costanzo, L.; Soto, C. S.; Tereshko, V.; Nanda, V.; Stayrook, S.; DeGrado, W. F. *Nature* **2008**, *451*, 596–599.
(32) Schnell, J. R.; Chou, J. J. *Nature* **2008**, *451*, 591–595.
(33) Hu, J.; Asbury, T.; Achuthan, S.; Li, C.; Bertram, R.; Quine, J. R.; Fu, R.; Cross, T. A. *Biophys. J.* **2007**, *92*, 4335–4343.
(34) Wang, J.; Kim, S.; Kovacs, F.; Cross, T. A. *Protein Sci.* **2001**, *10*, 2241–2250.
(35) Cady, S. D.; Hong, M. *Proc. Natl. Acad. Sci. U.S.A* **2008**, *105*, 1483–1488.
(36) Cady, S. D.; Mishanina, T. V.; Hong, M. *J. Mol. Biol.* **2009**, *385*, 1127–1141.

^{13}C chemical shifts, we predict the dominant rotameric states of five Val and Leu residues in M2TMP when bound to the lipid bilayer and compare them with the PDB structures obtained from other methods.

Materials and Methods

M2TMP Membrane Sample Preparation. The M2 transmembrane peptide of the Udorn strain of influenza A virus was synthesized by PrimmBiotech (Cambridge, MA) and purified to >95% purity. The amino acid sequence is SSDPL VVAASII GILHLIL WILDRL. Two peptide samples with different sets of uniformly ^{13}C, ^{15}N-labeled residues were used in this study. The first sample contains ^{13}C,^{15}N-labeled residues at V28, S31, and L36 (VSL-M2TMP). The second sample contains ^{13}C,^{15}N labels at V27, A30, I33, and L38 (VAIL-M2TMP). The peptide was reconstituted into DLPC lipid vesicles by detergent dialysis as described before,[36,37] with a peptide/lipid molar ratio of 1:15. A pH 7.5 phosphate buffer was used for the membrane sample preparation, thus the peptide studied here corresponds to the closed state of the proton channel. Both apo and amantadine-bound M2TMP were used. For the latter, amantadine was incorporated into the membrane by using buffer solutions containing 10 mM amantadine.

Solid-State NMR Experiments. SSNMR experiments were carried out on a Bruker AVANCE-600 (14.1 T) spectrometer and a DSX-400 (9.4 T) spectrometer (Karlsruhe, Germany). Triple-resonance MAS probes with 4 mm spinners were used, and samples were spun between 5 and 7 kHz. Typical rf pulse lengths were 5 μs for ^{13}C and 3.5−4.0 μs for ^{1}H. ^{1}H TPPM[38] or SPINAL[39] decoupling fields of 60−70 kHz were applied. ^{13}C chemical shifts were referenced to the α-Gly C′ signal at 176.49 ppm on the TMS scale.

Three 2D ^{13}C−^{13}C correlation experiments were used to measure and assign the methyl ^{13}C chemical shifts in M2TMP. The 2D DARR spin-diffusion experiment was carried out with a 10 ms mixing period under 5.333 kHz MAS. The double-quantum (DQ) filtered SQ−SQ experiment was carried out under 7 kHz MAS. The 2D dipolar-mediated INADEQUATE-type experiment was carried out under 7 kHz MAS. For the latter two experiments, ^{13}C−^{13}C dipolar recoupling was achieved using the SPC5 sequence.[40] All spectra were measured at 243 K where the peptide motion is frozen.

Statistical Analysis of Methyl Chemical Shifts and Side Chain Rotameric Conformation. To identify any potential correlation between the methyl ^{13}C chemical shifts and side chain conformation of Val and Leu, we searched the Biological Magnetic Resonance Data Bank (BMRB) and first-hand literature reports for stereospecifically assigned methyl ^{13}C chemical shifts. Most residues (62 out of 73) in α-helices were stereospecifically assigned, with an ambiguity value of 1 in the BMRB. The exceptions are two residues from Dcp2, where no ambiguity value was given, five residues from chicken cytochrome *c*, and two residues each from cofilin and fasciclin, which were assigned an ambiguity value of 2 (Table 2). The chemical shifts of these nonstereoassigned methyl groups fall within the general trend of each class and, therefore, were included in the analysis. The structures of proteins with available methyl chemical shifts were downloaded from the RCSB Protein Data Bank (PDB) and visualized in Insight II (Accelrys, Inc. San Diego). A total of 19 protein structures were examined, 17 of which were solved by solution NMR and 2 structures (profilin IIa and yeast cytochrome *c*) were solved by X-ray crystallography.

Table 1. Experimental Val and Leu Methyl ^{13}C Chemical Shifts (ppm)[a] in Apo and Amantadine-Bound (amt) M2TMP in DLPC Bilayers

Val		$\delta_{C\gamma 2}$	$\delta_{C\gamma 1}$	$\lvert\delta_{C\gamma 2} - \delta_{C\gamma 1}\rvert$	rotamer[b]
V27	apo	21.2	19.3	1.9	*t*
	amt	20.8	19.5	1.3	*t/m*
	soln NMR[c]	22.9	21.3	1.6	
V28	apo	20.7	19.5	1.2	*t/m*
	amt	20.8	19.0	1.8	*t*
	soln NMR[c]	22.7	21.4	1.3	
Leu		$\delta_{C\delta 1}$	$\delta_{C\delta 2}$	$\lvert\delta_{C\delta 1} - \delta_{C\delta 2}\rvert$	rotamer[b]
L26	apo	23.8	21.2	2.6	*mt*
	amt	23.3	20.9	2.4	*mt*
	soln NMR[c]	24.7	24.0	0.7	
L36	apo	24.2	21.2	3.0	*mt*
	amt	23.8	21.2	2.6	*mt*
	soln NMR[c]	23.4	24.9	1.5	
L38	apo	24.2	20.1	4.1	*mt*
	amt	23.9	21.0	2.9	*mt*
	soln NMR[c]	25.2	24.2	1.0	

[a] Solid-state NMR ^{13}C chemical shifts were not stereospecifically assigned and were measured at 243 K. The chemical shifts are referenced to TMS. [b] Predicted rotameric states based on the ^{13}C solid-state NMR chemical shifts. [c] Solution NMR methyl ^{13}C shift differences were measured on DHPC micelle bound M2(18−60) at ambient temperature.[32]

Table 2. Proteins that were Examined for Investigating the Conformational Dependence of Methyl ^{13}C Chemical Shifts in Proteins

protein	PDB ID	BMRB ID
ubiquitin	1d3z	4375
calmodulin, N-terminus	1f70	4056
calmodulin, C-terminus	1f71	4056
cytochrome *c*, chicken	2frc	1404
GB1	2gb1	7280
cofilin	1q8g	6004
profilin I	1pfl	4082
profilin IIa	2v8c	15452
fasciclin-like protein	1w7d	6312
talin C-terminal domain	2jsw	15411
Dcp2 decapping enzyme	2jvb	7325
M2 (residues 23−60)	2rlf	ref 32
RNase T_1	1ygw	ref 21
P22 c2 repressor	1adr	ref 18
malate synthase G	2jqx	ref 22
cytochrome *c*, yeast	2ycc	ref 14
phosphohistidine phosphatase	2ai6	6625
OmpX	1q9f	ref 54
Hsc-70	1ckr	ref 55

The side chain χ_1 and χ_2 angles were measured as N−Cα−Cβ−Cγ1 and Cα−Cβ−Cγ1−Cδ1, respectively, in Insight II.

The Val and Leu methyl ^{13}C chemical shifts were grouped first according to the backbone conformation (helix or sheet), then according to the side chain rotamer categories. For Val, the main rotamers are *t* (**t**rans, $\chi_1 = 180°$), *m* (**m**inus, $\chi_1 = -60°$), and *p* (**p**lus, $\chi_1 = +60°$) (Figure 1a),[41] using the nomenclature of the Penultimate Rotameric Library.[42] For Leu, the main rotamers are *mt* ($\chi_1 = -60°$, $\chi_2 = 180°$), *tp* ($\chi_1 = 180°$, $\chi_2 = 60°$), and *tt* ($\chi_1 = \chi_2 = 180°$) (Figure 1b). Our analysis focuses on the difference between the two methyl ^{13}C chemical shifts, which are not affected by possible inconsistencies in chemical shift calibration and are

(37) Luo, W.; Mani, R.; Hong, M. *J. Phys. Chem. B* **2007**, *111*, 10825–10832.
(38) Bennett, A. E.; Rienstra, C. M.; Auger, M.; Lakshmi, K. V.; Griffin, R. G. *J. Chem. Phys.* **1995**, *103*, 6951–6958.
(39) Fung, B. M.; Khitrin, A. K.; Ermolaev, K. *J. Magn. Reson.* **2000**, *142*, 97–101.
(40) Hohwy, M.; Rienstra, C. M.; Jaroniec, C. P.; Griffin, R. G. *J. Chem. Phys.* **1999**, *110*, 7983–7992.
(41) Markley, J. L.; Bax, A.; Arata, Y.; Hilbers, C. W.; Kaptein, R.; Sykes, B. D.; Wright, P. E.; Wüthrich, K. *Pure Appl. Chem.* **1998**, *70*, 117–142.
(42) Lovell, S. C.; Word, J. M.; Richardson, J. S.; Richardson, D. C. *Proteins: Struct., Funct., Genet.* **2000**, 40.

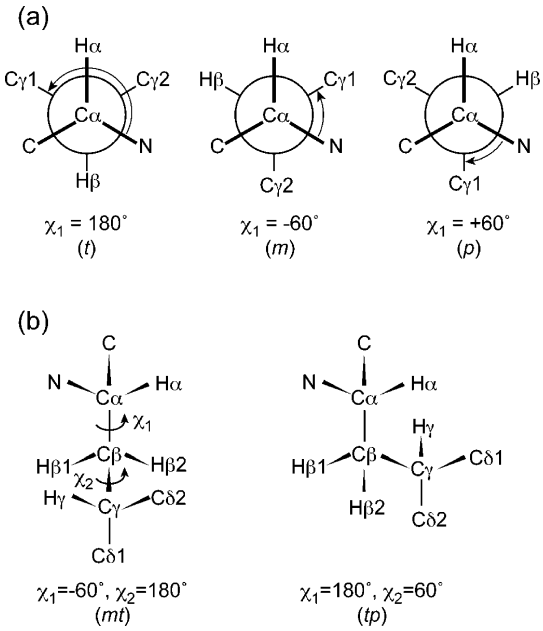

Figure 1. Definitions of the rotameric states of Val and Leu. (a) Val *t*, *m*, and *p* states. (b) Leu *mt* and *tp* states.

also less sensitive to ring current effects. The mean methyl chemical shift differences as well as the mean absolute shift differences are computed for each conformational category. The standard deviation σ of each distribution is calculated as

$$\sigma = \sqrt{\frac{1}{N-1}\sum_{i=1}^{N}(x_i - \bar{x})^2}$$

where x denotes the chemical shift difference. Chemical shift differences that fall beyond 2.6 times the standard deviations from the mean were discarded. This corresponds to a confidence level of 99% that these data points are anomalous or may be due to incorrect assignment. To obtain a measure of the uncertainty of the mean, we also computed the standard deviation of the mean $\sigma_{\bar{x}}$ as $\sigma_{\bar{x}} = \sigma/\sqrt{N}$.

Results and Discussion

Accurate Measurement of the Methyl ^{13}C Chemical Shifts. We first compare the relative merits of three 2D $^{13}C-^{13}C$ correlation experiments for accurate measurement of the methyl ^{13}C chemical shifts. The first experiment correlates SQ and SQ coherences and establishes the coherence transfer by ^{13}C spin diffusion. This DARR experiment[25] is the solid-state analogue of the solution NMR NOESY experiment. The second experiment correlates SQ coherences after passing them through a DQ filter, so that only ^{13}C sites involved in coupled spin networks are detected. This DQ-filtered SQ−SQ experiment is the solid-state analogue of the DQF-COSY experiment. The third experiment correlates the dipolar-generated DQ coherence with SQ coherence, thus it is analogous to the INADEQUATE experiment.[28] While all three solid-state MAS experiments are well-known, for clarity and comparison, we show their pulse sequences in Figure 2. The DQ excitation and reconversion periods are executed back-to-back between the evolution and detection periods of the DQ-filtered SQ−SQ experiment but are separated by the evolution period in the dipolar INADEQUATE (DQ−SQ correlation) experiment. The $^{13}C-^{13}C$ dipolar couplings for exciting the DQ coherences were recoupled

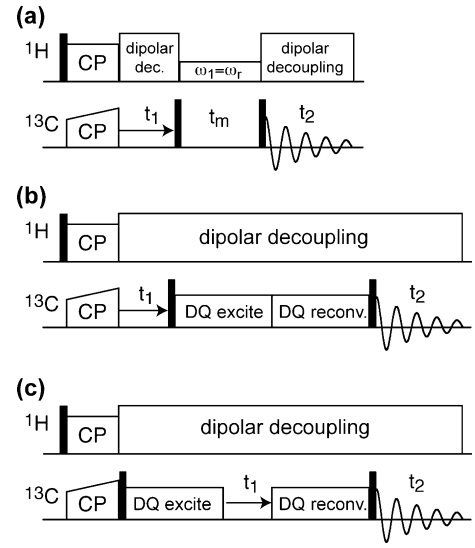

Figure 2. Pulse sequences for 2D $^{13}C-^{13}C$ correlation spectroscopy. (a) SQ−SQ correlation by DARR mixing. (b) DQ-filtered SQ−SQ correlation. (c) DQ−SQ correlation. The DQ excitation and reconversion are achieved by the SPC5 recoupling scheme.[40]

with the SPC5 sequence,[40] one of many recoupling sequences available.[43,44]

Figure 3 shows the three 2D correlation spectra of V28-, S31-, and L36-labeled M2TMP in DLPC bilayers at 243 K. The spin system connectivities are indicated in each spectrum. In the 2D DARR spectrum (a), the main resolved lipid signals along the diagonal are indicated with asterisks. It can be seen that while the Cα/Cβ cross peaks of the peptide are well-resolved in the spectrum the side chain cross peaks, especially those involving methyl groups, cluster near and overlap significantly with the diagonal. They include the L36 Cδ signal at 20.9 ppm and the V28 Cγ signal near 19.5 ppm (d). The homogeneous linewidths of the membrane sample at this temperature are actually relatively narrow, as seen by the width of the narrow part of the diagonal ridge. Thus, the broad bulges along the diagonal indicate cross peaks that are poorly resolved from the diagonal. In particular, the Ser Cα and Cβ chemical shifts are known to be similar in α-helices,[45] thus the broad diagonal peak around 61 ppm is due to the diagonal Cα and Cβ peaks overlapping with the true Cα/Cβ cross peaks (g). Moreover, in the 60−70 ppm region where the Ser signals resonate, there are various lipid signals such as the headgroup Cα (59.7 ppm), the glycerol G1 (63.2 ppm), and G3 (63.9 ppm).

The 2D DQ-filtered SQ−SQ correlation experiment considerably simplifies the spectrum by removing all lipid natural abundance ^{13}C signals along the diagonal (Figure 3b). The Leu and Val methyl regions now show well-resolved peaks, as seen in Figure 3e. The L36 Cγ signal at 24.9 ppm is well-separated from one of the Cδ peaks at 21.3 ppm. However, the second Leu methyl Cδ peak remains ambiguous. On the basis of the chemical shift databases, the second Leu methyl carbon may resonate close to the Cγ peak and thus may not be resolved from the diagonal. For the Ser Cα/Cβ cross peaks (Figure 3h), the DQ-filtered SQ−SQ correlation spectrum shows a distinct

(43) Lee, Y. K.; Kurur, N. D.; Helmle, M.; Johannessen, O. G.; Nielsen, N. C.; Levitt, M. H. *Chem. Phys. Lett.* **1995**, *242*, 304–309.
(44) Kristiansen, P. E.; Carravetta, M.; van Beek, J. D.; Lai, W. C.; Levitt, M. H. *J. Chem. Phys.* **2006**, *124*, 234510.
(45) Zhang, H.; Neal, S.; Wishart, D. S. *J. Biomol. NMR* **2003**, *25*, 173–195.

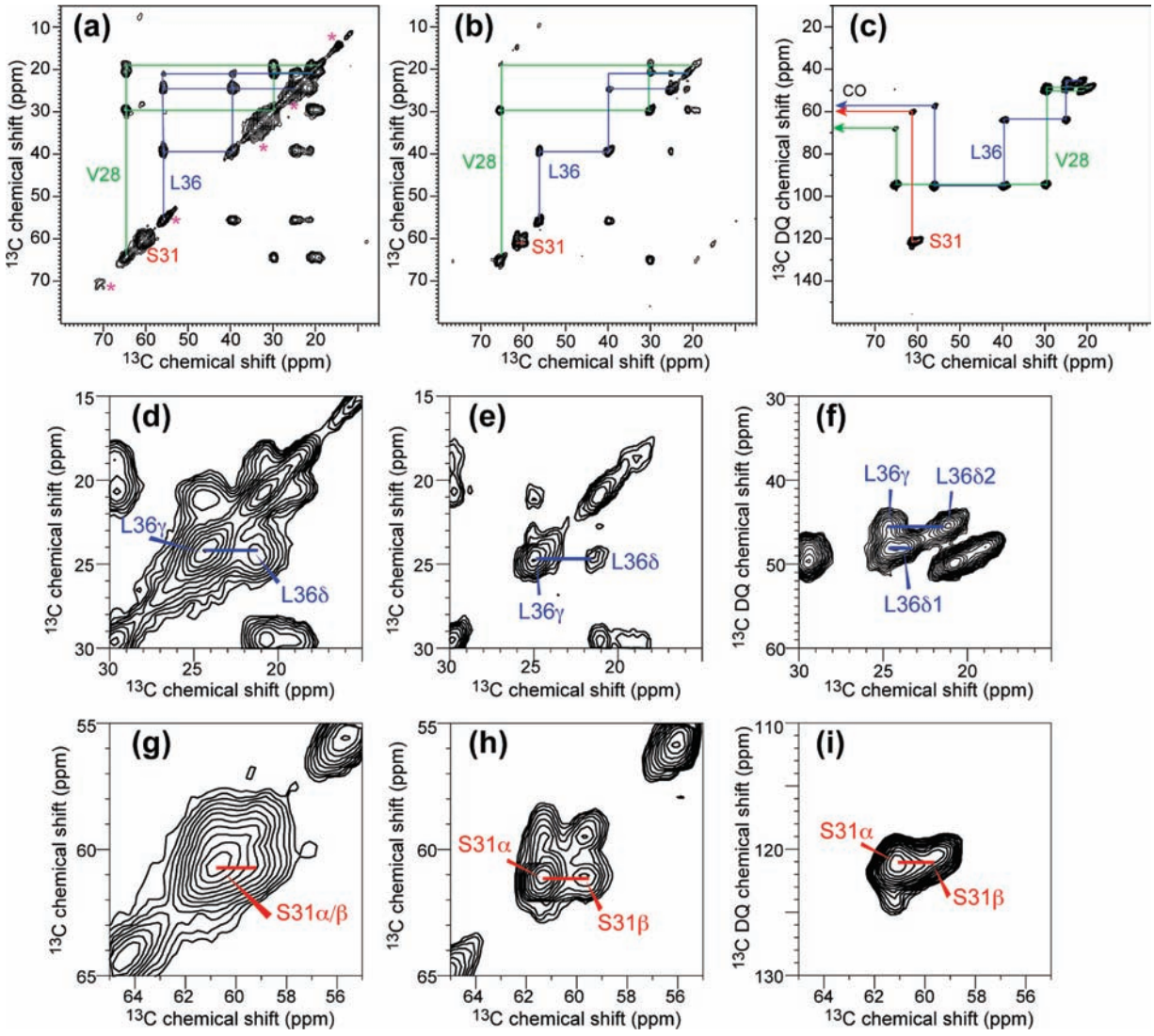

Figure 3. Two-dimensional $^{13}C-^{13}C$ correlation spectra of amantadine-complexed VSL-M2TMP in DLPC bilayers at 243 K. (a) Two-dimensional DARR spectrum with a 10 ms mixing time. (b) Two-dimensional DQ-filtered SQ−SQ correlation spectrum. (c) Two-dimensional DQ−SQ correlation spectrum. Two spectral regions are selected from each 2D spectrum and amplified in (d−i). Middle row (d−f): L36 methyl ^{13}C region. Bottom row (g−i): S31 Cα and Cβ region.

cloverleaf pattern, which gives a relatively clear Cα−Cβ chemical shift separation of 1.7 ppm. Further verification that the upfield peak is Cβ while the downfield peak is Cα can be made by a CH_2 filter experiment that suppresses all CH signals (thus Cα) while retaining all CH_2 signals (thus Cβ).[36]

The remaining ambiguity of the methyl ^{13}C chemical shifts is removed by the dipolar INADEQUATE experiment. Figure 3c shows the DQ−SQ correlation spectrum, and the expanded Leu methyl region is shown in Figure 3f. Now two Leu Cγ−Cδ correlation slices can be observed, with the upfield Cδ2 peak appearing in the 45.6 ppm DQ slice and the downfield Cδ1 peak appearing in the 48.3 ppm DQ slice. The latter is close to the Cγ peak near the slope-2 diagonal of the spectrum. Importantly, since there are no unpartnered diagonal peaks in the DQ−SQ correlation spectra, two coupled resonances that have nearly identical chemical shifts simply resonate near the slope-2 line of the spectrum and can be assigned unambiguously. In the case of VSL-M2TMP, since the L36 Cγ resonance is clearly resolved in the 45.6 ppm DQ slice to be 24.7 ppm, its partner Cδ1 peak can be readily read off in the 48.3 ppm DQ slice as the difference between 48.3 and 24.7 ppm, which is 23.6 ppm. Thus, the Cδ1 peak is only 1.1 ppm from the Cγ peak, which explains the difficulty of resolving the two peaks in the SQ−SQ correlation spectra (Figure 3a,b).

Figure 4 shows the three 2D spectra of VAIL-M2TMP in gel-phase DLPC bilayers. This sample contains three double-methyl residues (V27, I33, and L38), thus making their chemical shift identification difficult in the DARR spectrum. Specifically, the Val Cβ and Ile Cγ1 chemical shifts are very similar near 30 ppm, thus the Ile Cβ/Cγ1 cross peak (35.6, 28.4 ppm) is partly obscured by the Val Cβ peak and the lipid CH_2 diagonal peak (Figure 4d). Further, unless very long t_1 evolution times are used, the lipid CH_2 signal is often truncated, giving rise to truncation wiggles in the ω_1 dimension that interfere with the precise measurement of near-diagonal cross peaks. The long t_1 evolution times necessary for obtaining sharp lipid diagonal signals are usually excessive for the peptide signals, causing suboptimal use of the experimental time. The I33 Cγ1 signal at 28.4 ppm is also low and broad, which we attribute to the special spin dynamics of the Ile spin system. The two methyl groups of Ile have unequal distances from the backbone: the Cγ2 methyl group neighbors Cβ, while the Cδ methyl neighbors

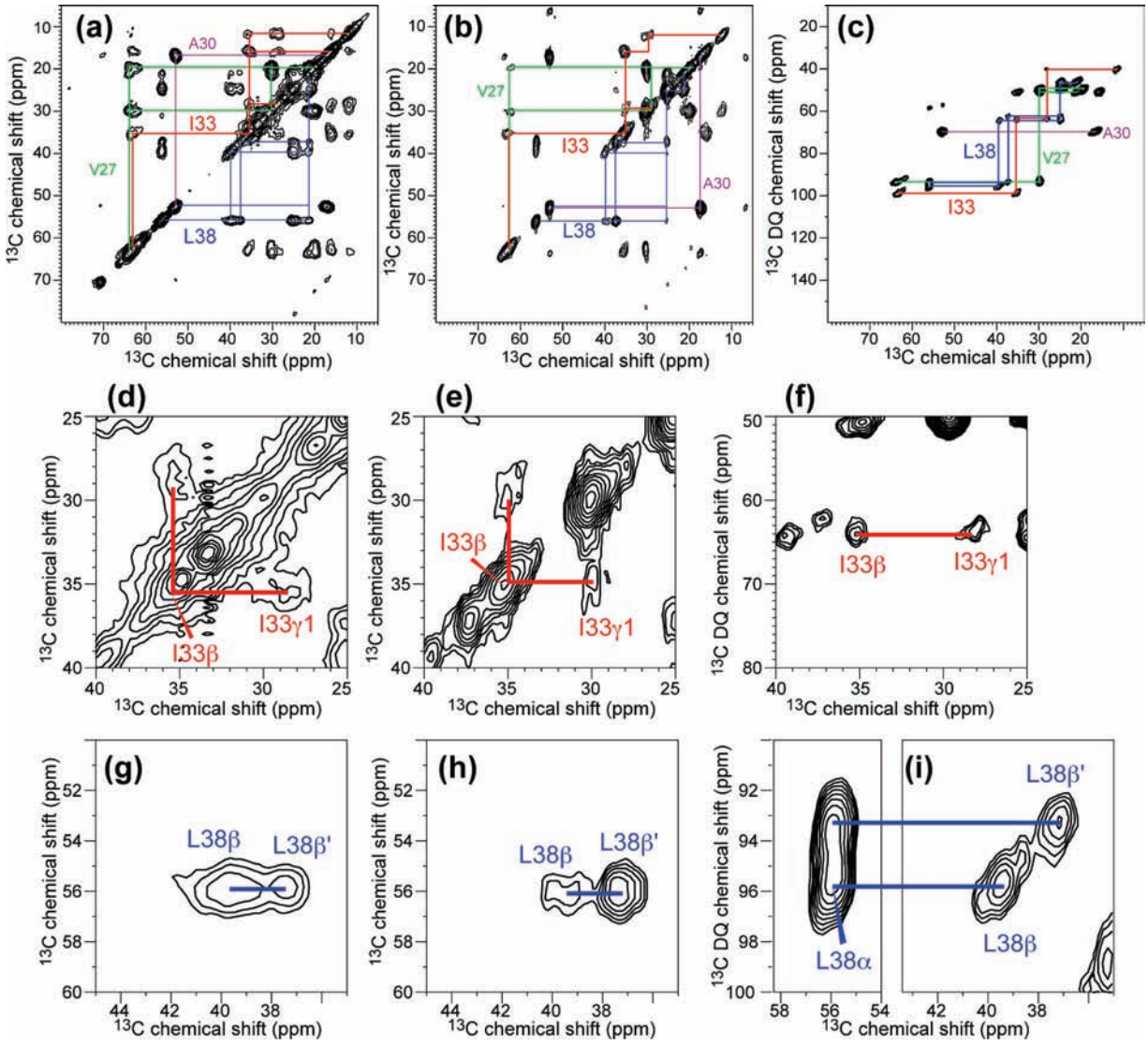

Figure 4. Two-dimensional $^{13}C-^{13}C$ correlation spectra of amantadine-complexed VAIL-M2TMP in DLPC bilayers at 243 K. (a) DARR spectrum with a 10 ms mixing time. (b) DQ-filtered SQ−SQ correlation spectrum. (c) DQ−SQ correlation spectrum. Two spectral regions are selected from each 2D spectrum in (a−c) and amplified in (d−i). Middle row (d−f): I33 Cβ−Cγ1 region. Bottom row (g−i): L38 Cα−Cβ region. Note the presence of two Cβ peaks.

Cγ1. The magnetization of Cγ1 between the two methyl groups appears to be disproportionally drawn to both methyl carbons, causing its low intensity in the 2D spectrum.

The DQ-filtered SQ−SQ correlation spectrum (Figure 4b,e) shows significantly simplified Ile Cβ/Cγ1 region: the cross peak, while still weak, can now be resolved from the diagonal since the lipid CH_2 peak is suppressed. However, the strong Val Cβ diagonal signal still remains. The DQ−SQ correlation spectrum (Figure 4c,f) gives the highest resolution for the Ile spin system. The two Cβ/Cγ1 cross peaks are now of similar intensities and have well-defined lineshapes and are well-resolved from the Val Cα/Cβ and Cβ/Cγ peaks. In addition, the methyl region of the spectrum is also much better resolved, similar to Figure 3.

Figure 4g−i demonstrates the ability of the dipolar INADEQUATE experiment to clearly identify conformational polymorphism. The L38 Cβ exhibits two chemical shifts that are 2.4 ppm apart. This is seen in all three 2D spectra but is most clearly manifested in the dipolar INADEQUATE spectrum since the presence of the two Cβ shifts is confirmed by the elongated shape of the Cα peak in the DQ dimension.

Methyl Chemical Shift Changes of M2TMP between the Apo and Amantadine-Bound States. The influenza A M2 transmembrane domain (residues 22−46) contains two Val residues (V27, V28), five Ile residues, and six Leu residues. We have labeled both Val residues and three of the Leu residues (L26, L36, and L38). Since the two Ile methyl carbons have chemical shift differences of about 5 ppm, their spectral identification usually does not pose any difficulty and will not be discussed further.

The binding of the M2 channel inhibitor amantadine has been recently shown to cause noticeable changes in the ^{13}C chemical shifts of various residues.[35,36] Here we focus on the methyl ^{13}C shift changes induced by the drug. Figure 5 compares the methyl regions of the five Val and Leu residues between the apo peptide and the amantadine-bound peptide. The DQ−SQ correlation spectra of Leu residues and the DARR spectra of Val residues are shown, the latter because the Val Cβ/Cγ cross peaks are sufficiently separated from the diagonal. Figure 5 shows that four out of five residues show methyl chemical shift perturbations by amantadine. Between the two Val residues, the V27

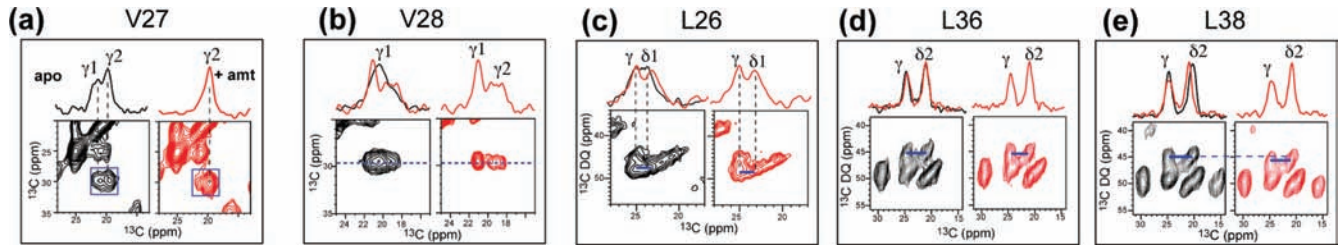

Figure 5. Methyl ^{13}C chemical shift changes of labeled Val and Leu residues in M2TMP in the absence (black) and presence (red) of amantadine. (a) V27 Cγ chemical shifts from 2D DARR spectra. (b) V28 Cγ chemical shifts from 2D DARR spectra. (c−e) Leu Cγ and Cδ chemical shifts from 2D DQ−SQ correlation spectra: (c) L26, (d) L36, (e) L38. Except for L36, all other residues show methyl ^{13}C chemical shift perturbations by amantadine.

Table 3. Statistics of Val and Leu Methyl ^{13}C Chemical Shift Differences from Protein Databases

Valine						
rotamer	population	no. residues	mean $\delta_{C\gamma 2} - \delta_{C\gamma 1}$ (ppm)	$\sigma_{\delta C\gamma 2 - \delta C\gamma 1}$ (ppm)	mean $\lvert\delta_{C\gamma 2} - \delta_{C\gamma 1}\rvert$ (ppm)	$\sigma_{\lvert\delta C\gamma 2 - \delta C\gamma 1\rvert}$ (ppm)
helix, *t*	90%	21	1.71 ± 0.12	0.52	1.67 ± 0.11	0.51
helix, *m*	7%	6	−1.23 ± 0.41	1.00	1.23 ± 0.41	1.00
sheet, *t*	72%	24	−0.26 ± 0.29	1.41	1.25 ± 0.14	0.65
sheet, *m*	20%	2	−1.95 ± 0.65	0.92	1.95 ± 0.65	0.92
sheet, *p*	8%	5	0.28 ± 1.07	2.39	1.76 ± 0.62	1.39

Leucine						
rotamer	population	no. residues	mean $\delta_{C\delta 1} - \delta_{C\delta 2}$ (ppm)	$\sigma_{\delta C\delta 1 - \delta C\delta 2}$ (ppm)	mean $\lvert\delta_{C\delta 1} - \delta_{C\delta 2}\rvert$ (ppm)	$\sigma_{\lvert\delta C\delta 1 - \delta C\delta 2\rvert}$ (ppm)
helix, *mt*	62%	15	2.89 ± 0.25	0.94	2.89 ± 0.25	1.13
helix, *tp*	30%	15	−0.10 ± 0.24	0.90	0.73 ± 0.13	0.50
helix, *tt*	1%	11	0.17 ± 0.35	1.15	0.90 ± 0.20	0.67
sheet, *mt*	46%	11	1.92 ± 0.32	1.01	2.12 ± 0.24	0.75
sheet, *tp*	36%	9	0.74 ± 0.77	2.30	2.14 ± 0.29	0.87

Cγ1 intensity is weakened by amantadine binding, whereas the V28 Cγ2 intensity is increased by amantadine binding. Among the three Leu residues, L36 exhibited no chemical shift changes, whereas the L26 Cδ1 and L38 Cδ2 frequencies are shifted from their apo values. Since our methyl ^{13}C assignments are not stereospecific, below we will use the absolute values of the methyl ^{13}C chemical shift differences extracted from the protein databases to interpret the conformation of these M2 side chains.

Table 1 lists the methyl ^{13}C chemical shifts of the five Val and Leu residues in the apo and amantadine-bound M2TMP in DLPC bilayers. Overall, amantadine causes 0.5−1.2 ppm changes in the methyl ^{13}C chemical shift difference. To interpret these ^{13}C chemical shift changes, we turn to an analysis of the methyl chemical shift trends in protein NMR databases.

Dependence of Val and Leu Methyl ^{13}C Chemical Shifts on Protein Side Chain Conformation. Methyl ^{13}C chemical shifts are sensitive to a number of factors, including the side chain conformation, which can manifest through *γ-gauche* effects,[46] and ring current effects. We hypothesize that, when ring current effects are excluded by considering methyl ^{13}C shift *differences* in each residue, the side chain conformation is the main determining factor for the methyl chemical shifts. Further, we wish to determine whether distinct trends of methyl ^{13}C chemical shifts exist for different side chain rotamers that are assigned by combinations of NOEs, RDCs, and scalar couplings. The existence of a significant correlation between the methyl chemical shifts and rotameric states would indicate that rotameric averaging, while present, is not too extensive to obliterate side chain conformational differences. We examined the methyl ^{13}C chemical shifts of 19 proteins in the RCSB Protein Data Bank, 17 of which are solution NMR structures and 2 are X-ray crystal structures. These proteins and their BMRB and PDB accession numbers are listed in Table 2. The rotameric states and methyl ^{13}C chemical shifts of the α-helical Val and Leu residues among these 19 proteins are listed in the Supporting Information Tables S1 and S2. It is important to note from the beginning that, since the conformational dependence is searched from solution NMR structures, any rotameric averaging necessarily reflects side chain dynamics in medium to large globular proteins in solution at ambient temperature. The extent of this averaging depends on the percentage of surface-accessible residues. However, our systems of interest are membrane proteins in lipid bilayers at low temperatures, which have very little or no rotameric averaging, thus their methyl chemical shifts would correspond to purer conformational states.

The rotameric states of proteins depend on the backbone conformation. α-Helical (H) and *β*-sheet (S) backbones have different populations of side chain conformations for steric reasons.[42] Thus, we first sort the methyl ^{13}C chemical shifts by the backbone conformation. Within each backbone category, we binned the methyl ^{13}C chemical shifts according to the canonical χ_1 and χ_2 angles. Since most solution NMR data we considered have stereospecifically assigned Val Cγ1/Cγ2 and Leu Cδ1/Cδ2 chemical shifts, we first analyzed the methyl ^{13}C chemical shift difference with the sign. However, because stereospecific assignment is still not possible by solid-state NMR, we also need to investigate whether the absolute value of the methyl ^{13}C chemical shift difference can serve to distinguish different rotamers. Thus Table 3 lists both the sign-sensitive and absolute methyl ^{13}C shift differences of Val and Leu in α-helical and *β*-sheet secondary structures. The standard deviations of the distributions are indicated, along with the standard deviations of the mean, which are reported as uncertainties (±) of the mean.

(46) Grant, D. M.; Paul, E. G. *J. Am. Chem. Soc.* **1964**, *86*, 2984–2990.

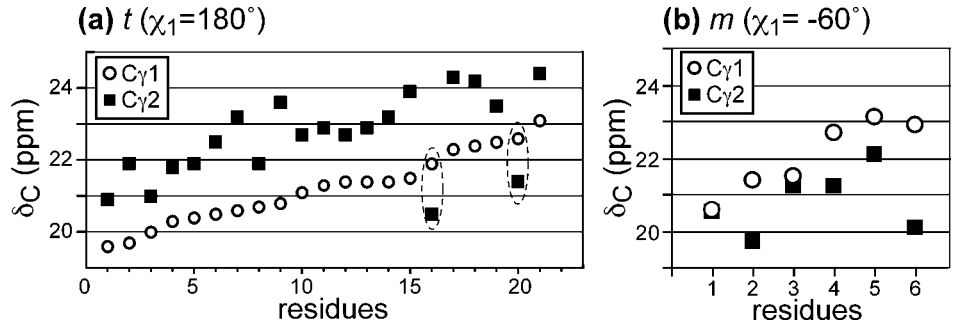

Figure 6. α-Helical Val Cγ chemical shifts as a function of side chain conformation from protein databases: (a) *t* rotamer; (b) *m* rotamer. Dashed lines in (a) indicate anomalous data points that are excluded in the statistical analysis in Table 3.

Figure 6 plots the α-helical Val Cγ1 and Cγ2 chemical shifts in the *t* and *m* rotamers. The *t* rotamer ($\chi_1 = 180°$) dominates (90%) in α-helical Val's and thus has the largest number of data points. It can be seen that the Cγ2 chemical shift is more downfield (larger) than the Cγ1 shift in most cases, with an average difference of 1.71 ppm and a standard deviation of 0.52 ppm. Only 2 out of 21 data points in this class have upfield Cγ2 chemical shifts than Cγ1. Because of the dominance of the *t* rotamer in Val and the generally downfield Cγ2 shifts, we calculate the methyl ^{13}C shift difference for Val as $\delta_{C\gamma 2} - \delta_{C\gamma 1}$. When the absolute value of the methyl shift differences is considered, the average difference is 1.67 ppm. This trend agrees qualitatively with the recent finding of London and co-workers based on a smaller sample size of five proteins.[15]

For the *m* rotamer of helical Val (7% abundant in proteins), the mean absolute Cγ2/Cγ1 shift difference is about 0.5 ppm smaller than the *t* rotamer. More importantly, the sign of the chemical shift difference is reversed, with the Cγ1 chemical shifts now more downfield than Cγ2. Thus, new SSNMR techniques for stereospecific assignment of the Val methyl ^{13}C chemical shifts should be able to distinguish the *t* and *m* rotamers simply based on the relative values of the Cγ1 and Cγ2 shifts. The upfield Cγ2 shift in the *m* rotamer can be well explained by the *γ-gauche* effect, as the Cγ2 carbon is *gauche* to both the N and C′ atoms of the backbone (Figure 1a) and experiences steric crowding.[15,46] For the *p* rotamer, due to its very low occurrence in proteins (2%) and the small chemical shift sample size (5 points) we found from databases, we do not consider its methyl chemical shift trend further.

Figure 7 shows the Cδ1 and Cδ2 chemical shifts of α-helical Leu residues. For the dominant *mt* rotamer (62%), the stereospecifically assigned Cδ1 chemical shifts are uniformly more downfield than Cδ2, with an average difference, $\delta_{C\delta 1} - \delta_{C\delta 2}$, of 2.89 ppm and a standard deviation of 0.94 ppm (Table 3). The upfield Cδ2 chemical shift in this rotamer can again be understood by the steric crowding of Cδ2 to Cα through the *γ-gauche* effect, as visualized in Figure 1b. In contrast, the 30% abundant *tp* rotamer has a much smaller absolute methyl shift difference of 0.73 ppm and has no clear trend in which methyl carbon has larger chemical shifts. Given the significant difference in the absolute methyl shift differences, these two most populated Leu rotamers can be readily distinguished even without stereospecific assignment.

For *β*-sheet backbones, the Val methyl shift differences are larger for the *m* rotamer than the *t* rotamer, contrary to the trend of the helical Val's, although only a small data set is available for the *m* rotamer. For *β*-sheet Leu's, the *tp* rotamer has as many positive as negative methyl ^{13}C shift differences, thus is ambiguous to distinguish from the *mt* rotamer.

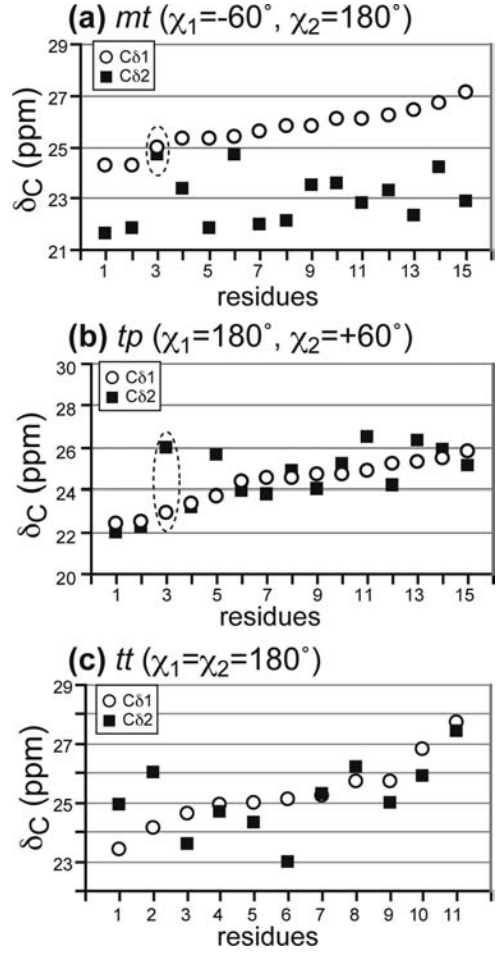

Figure 7. α-Helical Leu Cδ methyl chemical shifts as a function of side chain conformation from protein databases: (a) *mt* rotamer; (b) *tp* rotamer; (c) *tt* rotamer. Dashed lines in (a) and (b) indicate anomalous data points that are not included in the statistical calculation in Table 3.

The recent work of London and co-workers considered the side chain ^{13}C chemical shifts of not only the three double-methyl residues but also six other residues in five proteins.[15] The main finding of the paper is that steric crowding by *gauche* conformations of Cγ substituents causes upfield shifts of the Cγ resonances. The paper reached qualitatively similar conclusions about the methyl ^{13}C shift differences of Val and Leu as the present work. However, many quantitative details differ, mainly due to the fact that the previous work did not distinguish the α-helical and *β*-sheet backbone conformation, which are found here to give significantly different Cγ and Cδ shift differences. For example, while the Val *t* rotamer has much

more upfield Cγ1 shifts than Cγ2 in α-helices (Table 3), the average difference is much smaller in β-sheets (−0.26 ppm) due to crossover of the Cγ2 and Cγ1 shifts. Another example is the Leu *tp* rotamer, which shows very different average Cδ shift differences between the helical and sheet conformations (Table 3). Thus, mixing of helical and sheet rotamers obscures some chemical shift trends. Expressed in terms of the chemical shift of a certain carbon in different rotamers, we find that the Leu Cδ1 average shift difference between the *tp* and *mt* rotamers in α-helices is $\delta_{C\delta1,tp} - \delta_{C\delta1,mt} = -1.4$ ppm but has a much smaller value of −0.1 ppm in β-sheets. This suggests that steric crowding, which causes upfield shifts of the Cδ1 resonance, is stronger in α-helical *tp* rotamers than β-sheet *tp* rotamers. Second, the London work analyzed the χ_1 dependence of chemical shifts separately from the χ_2 dependence. For Leu, however, whose *mt* and *tp* rotamers are predominant and few other rotamers are populated, the combined χ_1/χ_2 analysis better reflects the conformational dependence of methyl chemical shifts.

How significant is the effect of rotameric averaging, which occurs more commonly in surface-accessible residues than interior residues in globular proteins, to the statistical methyl chemical shifts obtained here? To a first approximation, the fact that clear distinctions do exist between the methyl ^{13}C shift differences of the Leu and Val rotamers indicates that side chain conformational equilibria in globular proteins have sufficiently limited amplitudes or significantly skewed populations. Comparison of crystal structures with solution NMR structures showed that the solution NMR derived dominant rotamers generally agree well with the crystal structure.[21,24] Earlier studies of structural and fibrous proteins such as collagen,[47] keratin intermediate filaments,[48] and the coat protein of filamentous bacteriophages[49] by ^{2}H SSNMR found that Leu side chains interconvert rapidly between the *mt* and *tp* rotamers with nearly equal populations. This extensive rotameric averaging was thought to have functional importance, one example being the distribution of mechanical stresses experienced by collagen fibrils in the organic−inorganic nanocomposites of bone. In membrane proteins, Val side chain dynamics have been examined in bacteriorhodopsin[50] and gramicidin[51] by ^{2}H SSNMR, with the former showing no χ_1 dynamics at all and the latter showing χ_1 averaging for some of the Val residues but with a dominant rotamer. While the literature of membrane protein side chain dynamics is still limited, it is reasonable to hypothesize that small membrane peptides would exhibit more extensive side chain conformational motion than large membrane proteins. Compared to fibrous and membrane proteins, large globular proteins have relatively small surface areas, thus near-equal populations of rapidly interconverting rotamers should be much less common, which explains the current statistical findings. In any case, since the methyl shift trends found here likely correspond to partially averaged conformational states, the true chemical shift differences between pure rotamers will be more pronounced than given here. Therefore, solid-state NMR methyl chemical shifts measured at low temperature, where most χ_1 and χ_2 conformational dynamics are frozen, should show larger chemical shift differences between different rotamers.

Verification of the χ_1 Dependence of Val Methyl Chemical Shifts in M2TMP. On the basis of the above conformational dependence of methyl ^{13}C chemical shifts and the measured M2TMP Val and Leu ^{13}C chemical shifts, we can assign the rotameric states for the five Val and Leu residues. Table 1 shows that all three Leu residues should be assigned to the dominant *mt* rotamer, and amantadine binding, while changing the methyl shift differences by as much as 1.2 ppm, does not change the assignment of the canonical rotamer. The particularly large methyl shift difference of L38 (4.1 ppm) in the apo state of M2TMP likely corresponds to a purer or more ideal *mt* conformation compared to L26 and L36.

For the two Val residues, the apo V27 and amantadine-bound V28 can be readily assigned to the *t* rotamer. On the other hand, the amantadine-bound V27 and the apo V28 have smaller methyl ^{13}C shift differences of about 1.2 ppm that correlate better with the *m* rotamer (Table 3). However, because of the relatively small methyl shift difference between the *m* and *t* Val rotamers in the absence of sign information, such an assignment may not be definitive. Thus, we directly measured the χ_1 torsion angle of Val using the HCCH dipolar correlation experiment. This serves to verify the correlation between the methyl ^{13}C chemical shifts and rotameric states of Val. This direct measurement is possible for Val because its Cβ is a branched CH group with a single proton, so that correlation of the orientation-dependent Cα−Hα and Cβ−Hβ dipolar couplings gives the relative orientation of the two C−H bonds, which is the χ_1 angle.

Figure 8a shows the pulse sequence of the HCCH experiment, which differs from the original experiment[7] in the choice of the DQ dipolar recoupling sequence and in the dipolar-doubled nature of the C−H evolution period. We used the narrow-band HORROR recoupling scheme,[52] where the ^{13}C irradiation field ω_1 is matched to half the spinning frequency ω_r, to selectively recouple the Val Cα and Cβ signals. This eliminates possible contribution of the Val Cγ−Hγ dipolar coupling to the Hα−Cα−Cβ−Hβ dipolar correlation curve. Figure 8b shows the first slice of the V28 HCCH 2D spectrum, indicating the clean selection of the Cα and Cβ signals. The dipolar doubling during the t_1 period is achieved by a constant time of one rotor period for homonuclear decoupling combined with moving ^{13}C 180° pulses to define the effective t_1 time.[53] This dipolar-doubled constant-time HCCH evolution both enhances the angular resolution of the χ_1 technique and removes possible T_2 relaxation effects during t_1.

Panels c and d display the time evolution of the two Val residues under the dipolar couplings for the apo (black) and amantadine-bound states. The unsymmetrized time domain data show little intensity asymmetry for the V27 data and only minor asymmetry for the V28 data, which is due to finite pulse length effects. For V27, the amantadine-bound peptide shows deeper dipolar dephasing than the apo state, indicating a smaller χ_1 angle. Simulations yielded a best-fit χ_1 angle of 164° for the apo peptide and 158° for the complexed peptide. Thus, amantadine binding shifts the χ_1 angle by 6° away from the *trans* conformation. This is consistent with the direction of change predicted by the methyl ^{13}C chemical shifts. For

(47) Batchelder, L. S.; Sullivan, C. E.; Jelinski, L. W.; Torchia, D. A. *Proc. Natl. Acad. Sci. U.S.A.* **1982**, *79*, 386–389.
(48) Mack, J. W.; Torchia, D. A.; Steinert, P. M. *Biochemistry* **1988**, *27*, 5418–5426.
(49) Colnago, L. A.; Valentine, K. G.; Opella, S. J. *Biochemistry* **1987**, *26*, 847–854.
(50) Kinsey, R. A.; Kintanar, A.; Tsai, M. D.; Smith, R. L.; Janes, N.; Oldfield, E. *J. Biol. Chem.* **1981**, *256*, 4146–4149.
(51) Lee, K. C.; Huo, S.; Cross, T. A. *Biochemistry* **1995**, *34*, 857–867.
(52) Nielsen, N. C.; Bildsoe, H.; Jakobsen, H. J.; Levitt, M. H. *J. Chem. Phys.* **1994**, *101*, 1805–1812.
(53) Hong, M.; Gross, J. D.; Rienstra, C. M.; Griffin, R. G.; Kumashiro, K. K.; Schmidt-Rohr, K. *J. Magn. Reson.* **1997**, *129*, 85–92.
(54) Hilty, C.; Wider, G.; Fernández, C.; Wüthrich, K. *J. Biomol. NMR* **2003**, *27*, 377–382.
(55) Hup, W.; Zuiderweg, E. R. P. *J. Magn. Reson.* **1996**, *113*, 70–75.

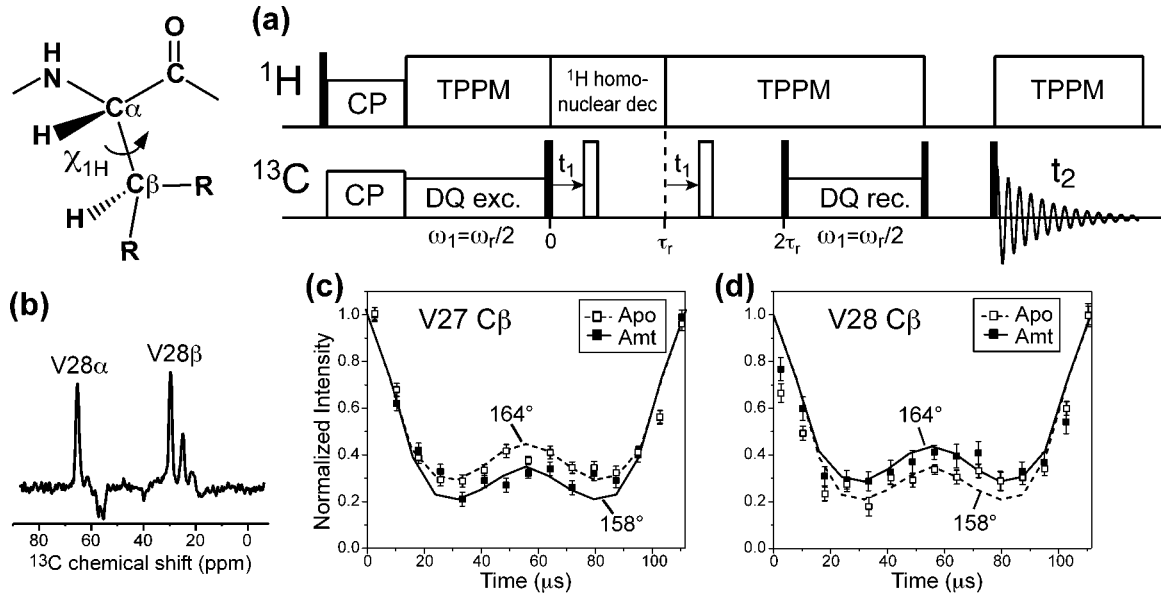

Figure 8. Direct measurement of the χ_1 torsion angles of V27 and V28 in M2TMP in the apo (open symbols) and amantadine-bound (filled symbols) states. (a) Double-quantum HCCH pulse sequence for correlating the H$\alpha-$Cα bond and H$\beta-$Cβ bond orientations to give the χ_{1H} angle, which is equal to the χ_1 = N$-$C$\alpha-$C$\beta-$Cγ angle. (b) ^{13}C chemical shift dimension of the HCCH spectra of V28-labeled M2TMP. Only the Val Cα and Cβ signals are selected. (c) Unsymmetrized V27 HCCH time-domain data for the apo peptide and the amantadine-complexed peptide. The best-fit χ_{1H} angle is indicated. The bound peptide shows a 6° decrease of the χ_{1H} angle, consistent with the direction of the chemical shift change. (d) Unsymmetrized V28 HCCH data. The bound peptide has a 6° higher χ_{1H} angle than the apo peptide, consistent with the direction of the chemical shift change.

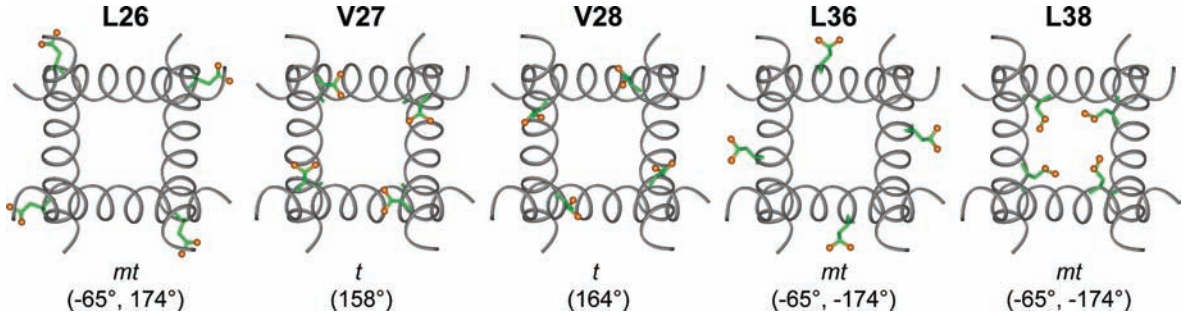

Figure 9. Rotameric states of Val and Leu residues determined by methyl ^{13}C chemical shifts and direct χ_1 angle measurements in amantadine-bound M2TMP. The backbone structure is for the amantadine-bound peptide[36] (PDB accession code: 2kad).

V28, the opposite change is observed: the amantadine-bound peptide has shallower dipolar dephasing, giving a χ_1 angle that is 6° larger, or *closer* to the *trans* conformation, compared to the apo peptide. This difference is again consistent with the methyl chemical shift predictions. In addition to the consistent direction of change between the apo and bound samples for each Val residue, the HCCH data are in quantitative agreement with the methyl shift differences between V27 and V28. Namely, the V27 apo sample and the V28 bound state, which have similar methyl shift differences of 1.9 and 1.8 ppm, have the same HCCH$-\chi_1$ angle of 164°. The V27 bound state and the V28 apo state, which have similar methyl shift differences of 1.3 and 1.2 ppm, also have the same HCCH$-\chi_1$ angle of 158°. Thus, direct torsion angle experiments bear out the chemical-shift-based prediction of the *t* and *m* rotamers in all four cases (Table 1).

Figure 9 shows the rotameric states of the five Val and Leu residues in amantadine-bound M2TMP in top views of the helical bundle. All three Leu residues have the *mt* rotamer, while both Val residues have the *t* rotamer. Among these five residues, L36 has the most lipid-facing location, while L38 places its methyl groups closest to the channel lumen. L26 side chain has a more interfacial position. The two recent high-resolution structures of M2TMP differed on the rotameric states of various Leu residues. For example, the solution NMR structure shows a L26 rotamer of *tp*,[32] while the crystal structure shows a mixture of *mt* and *tp* states for L26.[31] The rotameric difference between the solution NMR structure and solid-state NMR structure appears to be real, as the solution NMR methyl ^{13}C chemical shift differences of the three Leu residues are significantly smaller than found by solid-state NMR here (Table 1). This probably results from a combination of the higher temperature of the solution NMR experiments, which favor rotameric averaging, and the use of detergent micelles in the solution NMR experiments, which may lead to different side chain conformations than in lipid bilayers.

Conclusion

We have shown that a significant statistical correlation exists between the methyl ^{13}C chemical shift differences of Leu and Val and their side chain conformations. For α-helical Val's, the *t* rotamer has more upfield Cγ1 shifts than Cγ2, while the *m* rotamer has more upfield Cγ2 shifts than Cγ1. For α-helical Leu's, the *mt* rotamer has a large methyl shift difference of 2.9 ppm while the *tp* rotamer only has an absolute methyl shift

difference of 0.73 ppm. Thus, accurate measurement of the methyl ^{13}C chemical shifts in membrane proteins, by means of 2D DQ−SQ correlation experiments, can help to determine and refine the side chain conformation of these proteins. Application to the influenza A M2 proton channel shows that two Val's adopt the dominant *t* rotamer while three Leu residues exhibit the dominant *mt* rotamer. This work indicates that protein solid-state NMR can play an important role in understanding the conformational dependences of side chain ^{13}C chemical shifts due to the ability to suppress rotameric averaging at low temperature. The solid-state NMR measured side chain chemical shifts can also serve as important benchmarks for further computational analysis of the conformation dependence of side chain chemical shifts.

Acknowledgment. This work is funded by National Science Foundation Grant MCB-0543473.

Supporting Information Available: Compiled Val and Leu methyl ^{13}C chemical shifts and the assigned rotamers are tabulated. This material is available free of charge via the Internet at http://pubs.acs.org.

JA901550Q